Electrorotation of a pair of spherical particles

J. P. Huang,[1] K. W. Yu,[1] and G. Q. Gu[1,2]
[1]*Department of Physics, The Chinese University of Hong Kong, Shatin, NT, Hong Kong*
[2]*Information College, East China Normal University, Shanghai 200 062, China*
(Received 26 July 2001; published 3 January 2002)

We present a theoretical study of electrorotation (ER) of two spherical particles under the action of a rotating electric field. When the two particles approach and finally touch, the mutual polarization interaction between the particles leads to a change in the dipole moment of the individual particle and hence the ER spectrum, as compared to that of the well-separated particles. The mutual polarization effects are captured by the method of multiple images. From the theoretical analysis, we find that the mutual polarization effects can change the characteristic frequency at which the maximum angular velocity of electrorotation occurs. The numerical results can be understood in the spectral representation theory.

DOI: 10.1103/PhysRevE.65.021401 PACS number(s): 82.70.−y, 77.22.Gm, 77.84.Nh

I. INTRODUCTION

When a suspension of colloidal particles or biological cells is exposed to an external electric field, the analysis of the frequency-dependent response yields valuable information on various processes, like the structural (Maxwell-Wagner) polarization effects [1,2]. For most substances, the permittivity and conductivity are only constant over a limited frequency range. The general tendency is for permittivity to decrease, and conductivity to concomitantly increase, in a series of steps as frequency increases. These step changes are called dispersions.

While the frequency-dependent response of biological cells can be investigated by the method of dielectric spectroscopy [3], conventional dielectrophoresis and electrorotation (ER) analyze the frequency dependence of translations and rotations of single particles in an inhomogeneous and rotating external field, respectively [4,5]. With the recent advent of experimental techniques such as automated video analysis [6] as well as light-scattering methods [2], the motion of particles can be accurately monitored. In ER, the rotating field induces a cell dipole moment which rotates at the angular frequency of the external field. Any dispersion process causes a spatial phase shift between the induced dipole moment and the external field vector, giving rising to a torque which causes the rotation of individual cells [7].

In the dilute limit in which a small volume fraction of particles or cells are suspended in a medium while the particles are well separated, we can concentrate on the ER response of individual particles by ignoring the mutual interactions between the particles. However, if the suspension is nondilute, one may not ignore the interactions. Moreover, when the strength of the rotating electric field increases, the Brownian motion can be ignored and the polarized particles tend to aggregate along the rotating field even in the dilute limit.

As an initial model, we will consider a pair of interacting particles dispersed in a suspension. When the two particles approach and finally touch, the mutual polarization interaction between the particles leads to a change in the dipole moment of individual particles and hence the ER spectrum, as compared to that of the well-separated particles. We will present a theoretical study on the ER spectrum of two spherical particles in the presence of a rotating electric field, and capture the mutual polarization effects by the method of multiple images [8], recently developed to calculate the interparticle force between touching spherical particles.

II. MULTIPLE IMAGE METHOD FOR A PAIR OF DIELECTRIC SPHERES

We first consider an isolated spherical cell of complex permittivity $\tilde{\epsilon}_1=\epsilon_1+\sigma_1/(i\omega)$ dispersed in a suspension medium of $\tilde{\epsilon}_2=\epsilon_2+\sigma_2/(i\omega)$, where ω is the frequency of the external field $\vec{E}_0$, and $i=\sqrt{-1}$. If one applies a rotating electric field, there is in general a phase difference between the induced dipole moment and the applied field vector, and thus a net torque is acting on the cell. The spin friction (analogous to the Stokes drag for translational motions) causes a steady-state rotational motion. In this case, the dipole moment of the isolated cell $\tilde{p}$ is

$$\tilde{p}=\frac{1}{8}\tilde{\epsilon}_2 D^3 b E_0, \tag{1}$$

where $b=(\tilde{\epsilon}_1-\tilde{\epsilon}_2)/(\tilde{\epsilon}_1+2\tilde{\epsilon}_2)$ is the dipole factor, and D the diameter of the cell.

To account for the effect of multipole interaction on the electrorotation, we consider a pair of touching spherical cells at a separation R suspended in a medium. We will calculate the effect of multipole interaction on the dipole moment. For a rotating field, the total dipole moment of one cell of the pair is given by

$$\tilde{p}^*=\tilde{P}_T\langle\cos^2\theta\rangle+\tilde{P}_L\langle\sin^2\theta\rangle=\frac{1}{2}(\tilde{P}_T+\tilde{P}_L), \tag{2}$$

where θ is the angle between the dipole moment and the line joining the centers of the spheres. The average over all possible orientations of the cells gives a factor 1/2. In Eq. (2), $\tilde{P}_T(\tilde{P}_L)$ is the transverse (longitudinal) dipole moment, being perpendicular (parallel) to the line joining the centers of the spheres. The transverse and longitudinal dipole moments are given by [8]

 ©2002 The American Physical Society

$$\tilde{P}_L=\tilde{p}\sum_{n=0}^{\infty}(2b)^n\left(\frac{\sinh\alpha}{\sinh(n+1)\alpha}\right)^3,$$

$$\tilde{P}_T=\tilde{p}\sum_{n=0}^{\infty}(-b)^n\left(\frac{\sinh\alpha}{\sinh(n+1)\alpha}\right)^3,$$

where α satisfies the relation $\cosh\alpha=R/D$. For two touching particles, the dipole moment of a particle is given by

$$\tilde{p}^*=\frac{1}{8}\tilde{\epsilon}_2 D^3 b^* E_0, \tag{3}$$

where the dipole factor of a pair is given by:

$$b^*=\frac{8\tilde{p}^*}{\tilde{\epsilon}_2 D^3 E_0}=\frac{1}{2}b\left[\sum_{n=0}^{\infty}(2b)^n\left(\frac{\sinh\alpha}{\sinh(n+1)\alpha}\right)^3+\sum_{n=0}^{\infty}(-b)^n\left(\frac{\sinh\alpha}{\sinh(n+1)\alpha}\right)^3\right]. \tag{4}$$

It is known that the angular velocity of electrorotation of a particle is related to the dipole factor (b or b^*) as follows

$$\Omega=-F(\epsilon_2,\eta,E_0)\,\mathrm{Im}[\text{dipole factor}], \tag{5}$$

where F is a function of ϵ_2, the dynamic viscosity η of the medium, as well as the electric-field magnitude E_0, and $\mathrm{Im}[\cdots]$ denotes the imaginary part of $[\cdots]$. For a spherical particle, $F(\epsilon_2,\eta,E_0)=\epsilon_2 E_0^2/2\eta$. Regarding η, the spin friction expression suffices for an isolated particle. However, for two interacting particles, we must consider the more complicated suspension hydrodynamics.

III. SPECTRAL REPRESENTATION AND DISPERSION SPECTRUM

In a recent paper [9], we studied the dielectric behavior of cell suspensions by employing the Bergman-Milton spectral representation of the effective dielectric constant [10]. By means of the spectral representation, we derived the dielectric dispersion spectrum in terms of the electrical and structure parameters of the cell models. The spectral representation is a rigorous mathematical formalism of the effective dielectric constant of a composite material. The essence of the spectral representation is to define the following transformations. If we denote a complex material parameter

$$\tilde{s}=\left(1-\frac{\tilde{\epsilon}_1}{\tilde{\epsilon}_2}\right)^{-1}, \tag{6}$$

then the dipole factor b^* admits the general form

$$b^*=\sum_n\frac{F_n}{\tilde{s}-s_n}, \tag{7}$$

where n is a positive integer, i.e., $n=1,2,\ldots$, and F_n and s_n are the nth microstructure parameters of the composite material [10].

Thus, the spectral representation offers the advantage of the separation of material parameters (namely, the dielectric constant and conductivity) from the cell structure information, thus simplifying the study. From the spectral representation, one can readily derive the dielectric dispersion spectrum, with the dispersion strength as well as the characteristic frequency being explicitly expressed in terms of the structure parameters and the materials parameters of the cell suspension [9]. The actual shape of the real and imaginary parts of the permittivity over the relaxation region can be uniquely determined by the Debye relaxation spectrum, parametrized by the characteristic frequencies and the dispersion strengths. So, we can study the impact of these parameters on the dispersion spectrum directly. In what follows, we further express the dipole factor b and b^* in the spectral representation. The dipole factor b admits the form $b=F_1/(\tilde{s}-s_1)$ in the spectral representation, where $F_1=-1/3$ and $s_1=1/3$. For the dielectric dispersion spectrum, we further define two dimensionless real parameters [9]

$$s=(1-\epsilon_1/\epsilon_2)^{-1},\quad \text{and}\quad t=(1-\sigma_1/\sigma_2)^{-1},$$

where s and t are the dielectric and conductivity contrasts, respectively. After simple manipulations, Eq. (7) becomes

$$b=\frac{F_1}{s-s_1}+\frac{\delta\epsilon_1}{1+if/f_c}, \tag{8}$$

where f_c is the characteristic frequency, at which the maximum angular velocity of electrorotation occurs, and $\delta\epsilon_1$ is the dispersion magnitude [9]

$$\delta\epsilon_1=F_1\frac{s-t}{(t-s_1)(s-s_1)},$$

$$f_c=\frac{1}{2\pi}\frac{\sigma_2}{\epsilon_2}\frac{s(t-s_1)}{t(s-s_1)}. \tag{9}$$

Similarly, the dipole factor of a pair of interacting particles b^* can be rewritten in the spectral representation as

$$b^*=\sum_{m=1}^{\infty}\left(\frac{F_m^{(T)}}{\tilde{s}-s_m^{(T)}}+\frac{F_m^{(L)}}{\tilde{s}-s_m^{(L)}}\right), \tag{10}$$

where

$$F_m^{(T)}=F_m^{(L)}=-\frac{2}{3}m(m+1)\sinh^3\alpha e^{-(2m+1)\alpha},$$

$$s_m^{(T)}=\frac{1}{3}[1+e^{-(1+2m)\alpha}],\quad s_m^{(L)}=\frac{1}{3}[1-2e^{-(1+2m)\alpha}].$$

In the above derivation, we have used the identity

$$\frac{1}{\sinh^3 x}=\sum_{m=1}^{\infty}4m(m+1)e^{-(1+2m)x}.$$

We should remark that the spectral representation of b^* [Eq. (10)] is an exact transformation [11] of the multiple image

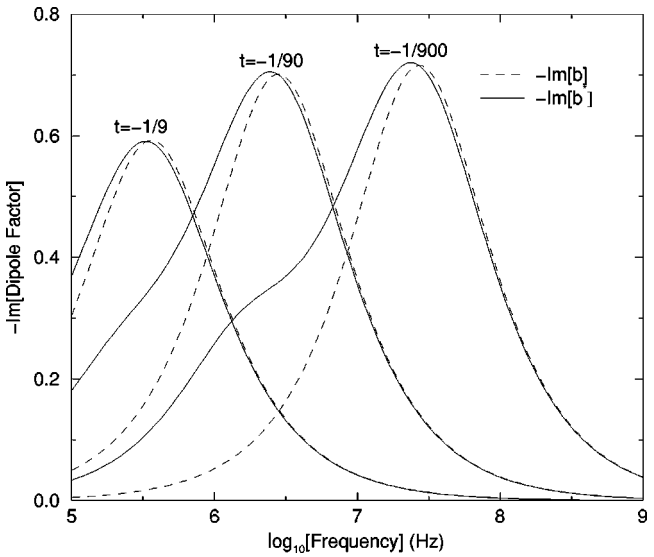

FIG. 1. The minus dipole factor (being proportional to the angular velocity of electrorotation) plotted vs frequency both for an isolated cell (dashed lines) and touching cells (solid lines) for three different conductivity contrasts t at $s=1.1$ and $\sigma_2=2.8\times10^{-4}$ Sm^{-1}.

expression [Eq. (4)]. Thus, the spectral representation of b^* consists of a discrete set of simple poles (see Fig. 5 below). The $m=1$ pole $s_1^{(L)}$ ($s_1^{(T)}$) for the longitudinal (transverse) field case deviates significantly from $s=1/3$, while $s_1^{(L)}$ becomes small in the touching limit $\alpha\to0$. In what follows, we will show that this pole gives a significant contribution to the ER spectrum at low frequency. As m increases, however, the series $s_m^{(T)}$ and $s_m^{(L)}$ accummulate to $s=1/3$, giving rise to a dominant contribution near the isolated-sphere frequency f_c. Moreover, each term in the spectral representation expression of b^* can be rewritten as

$$\frac{F_m^{(T)}}{\tilde{s}-s_m^{(T)}}=\frac{F_m^{(T)}}{s-s_m^{(T)}}+\frac{\delta\epsilon_m^{(T)}}{1+if/f_{mc}^{(T)}},$$

$$\frac{F_m^{(L)}}{\tilde{s}-s_m^{(L)}}=\frac{F_m^{(L)}}{s-s_m^{(L)}}+\frac{\delta\epsilon_m^{(L)}}{1+if/f_{mc}^{(L)}},$$

where $\delta\epsilon_m^{(T)}$ (or $\delta\epsilon_m^{(L)}$) and $f_{mc}^{(T)}$ (or $f_{mc}^{(L)}$) are the dispersion magnitudes and the characteristic frequencies of the transverse (longitudinal) field cases, obtained, respectively, by replacing F_1 and s_1 in the expressions of $\delta\epsilon_1$ and f_c in Eq. (9) with $F_m^{(T)}$ (or $F_m^{(L)}$) and $s_m^{(T)}$ (or $s_m^{(L)}$). Note that $f_{1c}^{(L)}$ is significantly lower than f_c. The ER spectrum of two spheres will consist of a series of subdispersions. In what follows, we will investigate the effect of multipole interaction on the electrorotation of cell, as shown in the next section.

IV. NUMERICAL RESULTS

For convenience, we let $F(\epsilon_2,\eta,E_0)=1$ in our numerical calculation, both for the isolated-particle and touching-particle cases, in order to study the effect of multipole interaction on the ER spectrum. It is because we will focus on the frequency dependence of the ER spectrum. On the other hand, we do not know the dynamic viscosity for two approaching spheres.

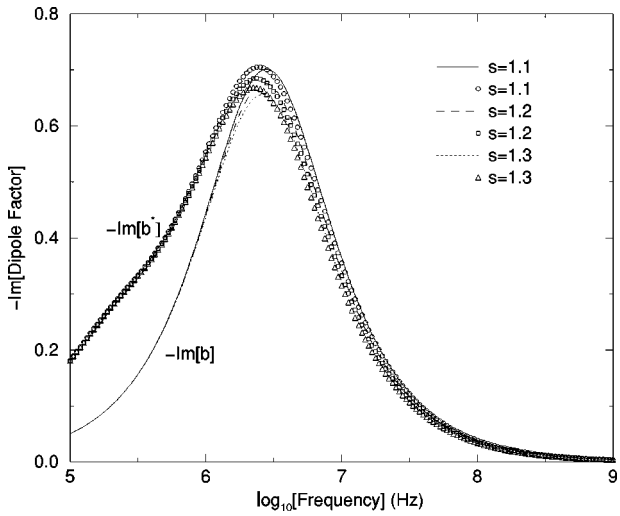

FIG. 2. Similar to Fig. 1 but for three different dielectric contrasts s at $t=-1/90$ and $\sigma_2=2.8\times10^{-4}$ Sm^{-1} for an isolated cell (lines) and touching cells (symbols).

Figure 1 is plotted to compare the two cases for three different conductivity contrast t. It is evident that, for both cases, a small $|t|$ yields a high-characteristic frequency, at which the peak locates. Moreover, a smaller $|t|$ gives a larger peak value. Given a constant t, the touching-cell case predicts a shift of the peak location to lower frequency than that predicted by the isolated-cell case. At the same time, the peak for the touching-cell case broadens. This behavior arises from the effect of the multipole interaction. In addition, if t is given, the two cases also predict different behavior within the low-frequency region, but almost the same behavior within the high-frequency region. Especially for small $|t|$ (e.g., $t=-1/900$), a second peak occurs at lower frequency. This is in accord with the prediction of the spectral representation.

Figure 2 is plotted to exhibit the effect of the material parameter s on the two cases. It is observed that, for both cases, a larger s gives a larger peak value. Moreover, the peak of different s appears at almost the same frequency for both cases. In summary, s may affect the peak value, but not the peak location.

Figure 3 is plotted for three different values of the medium conductivity σ_2 at $s=1.1$ and $t=-1/90$. For a larger σ_2, we get a larger characteristic frequency at which the peak occurs. It is evident that σ_2 may affect the peak location, but not the peak value.

In Fig. 4, as $R/D\approx1$ (e.g., $R/D=1.0333$), the deviation between the two cases is evident. In other words, the multipole interaction does play an important role in the ER spectrum and the effect cannot be neglected for touching particles. However, as the separation increases, say, $R/D=2$, both cases predicts the same ER spectrum. From the results, we would say that the effect of multipole interaction may be neglected at $R/D>2$.

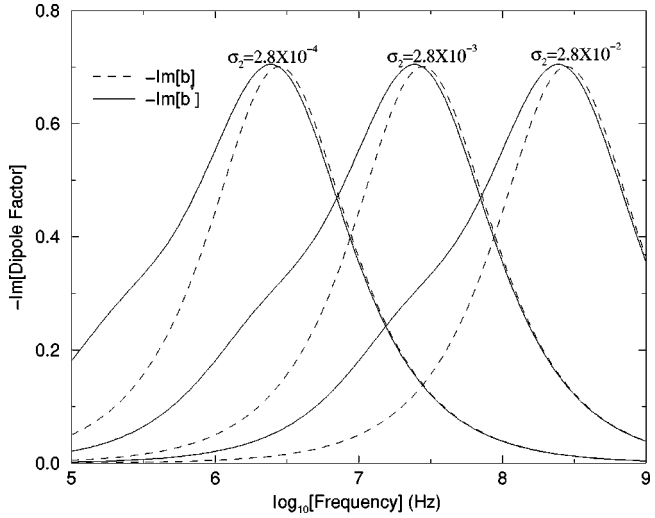

FIG. 3. Similar to Fig. 1 but for three different medium conductivities σ_2 at $s=1.1$ and $t=-1/90$.

In Fig. 5, we plot the spectral representation for the two sets of poles $s_m^{(L)}$ (or $s_m^{(T)}$) for $m=1$ to 100. As m increases, $s_m^{(L)}$ increases up to 1/3, while $s_m^{(T)}$ decreases towards 1/3. For small R/D ratio (say, $R/D=1.0333$), the longitudinal field plays a more important role in determining electrorotation spectrum than the transverse field. However, if R/D ratio is large enough, say, $R/D \geqslant 2$, (results not shown here), the effect of multipole interaction is negligible both for the longitudinal and transverse field cases and the results for an isolated cell recover. In summary, as the two cells approach and finally touch, one must take into account the effect of multipole interaction on the electrorotation of cells.

V. DISCUSSION AND CONCLUSION

Here, a few comments on our results are in order. In this work, we attempted a theoretical study of the electrorotation of two approaching spherical particles in the presence of a rotating electric field. When the two particles approach and finally touch, the mutual polarization interaction between the particles leads to a change in the dipole moment of individual particles and hence the ER spectrum, as compared to that of the well-separated particles. The mutual polarization effects are studied via the multiple image method. From the results, we find that the mutual polarization effects can change the characteristic frequency substantially. We should remark that the multiple image method for two dielectric spheres is only approximate [12], but the approximation is quite good [8]. More accurate calculations based on bispherical coordinates can be attempted. However, we believe that similar conclusions can be obtained.

Moreover, when the volume fraction of the suspension is large, the rotating electric field leads to platelike aggregation of particles in the plane of the applied field. In this case, the electrorotation spectrum can be modified further due to the local-field effects arising from the many-particle system. To this end, a first-principles approach can be used to handle the many-particle and multipole interactions [13].

Regarding the dynamic viscosity, the spin friction expression for an isolated spherical cell suffices. However, for many cells interacting in a suspension, we must consider the hydrodynamics. Regarding the dynamic viscosity for two touching spheres, we must consider the suspension hydrodynamics of two approaching spheres. This is a formidable task and should be a topic for future work.

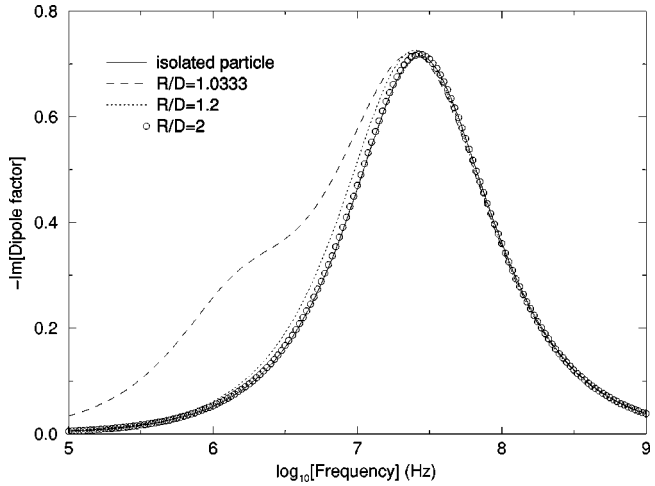

FIG. 4. Similar to Fig. 1 but for three different separation ratios R/D at $s=1.1$, $t=-1/900$, and $\sigma_2=2.8\times10^{-4}$ Sm^{-1}.

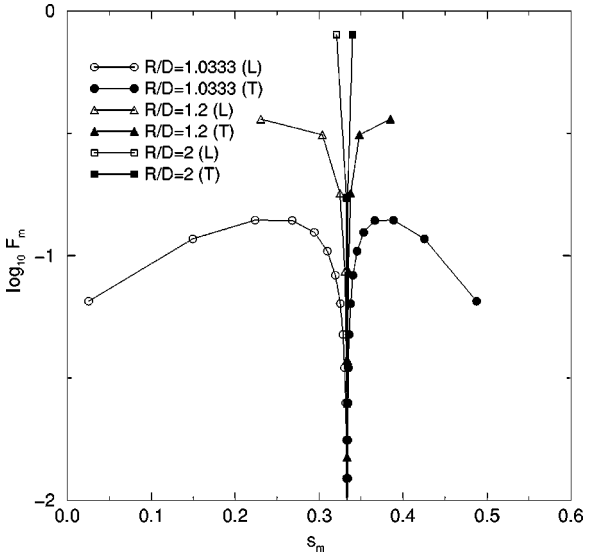

FIG. 5. The pole spectrum for two approaching spheres for several separation ratios R/D for the longitudinal (open symbols) and transverse (filled symbols) cases. Note that the longitudinal (transverse) part of the spectrum are on the small (large) s side of the spectrum. The lines are guides for the eyes.

ACKNOWLEDGMENTS

This work was supported by the Research Grants Council of the Hong Kong SAR Government under Grant No. CUHK 4245/01P. G.Q.G. acknowledges the financial support from a

Key Project of the National Natural Science Foundation of China under Grant No. 19834070. K.W.Y. acknowledges useful correspondence with Professor Mike Thorpe regarding the spectral representation of two approaching spheres, and extensive discussions with Professor Tuck Choy on the multiple image method.

[1] For a review, see J. Gimsa and D. Wachner, Biophys. J. **77**, 1316 (1999).
[2] J. Gimsa, Ann. N.Y. Acad. Sci. **873**, 287 (1999).
[3] K. Asami, T. Hanai, and N. Koizumi, Jpn. J. Appl. Phys. **19**, 359 (1980).
[4] G. Fuhr, J. Gimsa, and R. Glaser, Stud. Biophys. **108**, 149 (1985).
[5] J. Gimsa, P. Marszalek, U. Lowe, and T. Y. Tsong, Biophys. J. **73**, 3309 (1991).
[6] G. De Gasperis, X.-B. Wang, J. Yang, F. F. Becker, and P. R. C. Gascoyne, Meas. Sci. Technol. **9**, 518 (1998).
[7] J. P. H. Burt, K. L. Chan, D. Dawson, A. Parton, and R. Pethig, Ann. Biol. Clin. **54**, 253 (1996); see also http://www.ibmm.informatics.bangor.ac.uk/pages/science/rot.htm for the basic science of electrorotation.
[8] K. W. Yu and Jones T. K. Wan, Comput. Phys. Commun. **129**, 177 (2000).
[9] Jun Lei, Jones T. K. Wan, K. W. Yu, and Hong Sun, Phys. Rev. E **64**, 012 903 (2001).
[10] D. J. Bergman, Phys. Rep. **43**, 379 (1978).
[11] M. F. Thorpe (private communications); see also B. R. Djordjevic, J. H. Hetherington, and M. F. Thorpe, Phys. Rev. B **53**, 14 862 (1996) for a similar method in two dimensions.
[12] T. C. Choy, A. Alexopoulos, and M. F. Thorpe, Proc. R. Soc. London, Ser. A **454**, 1993 (1998).
[13] K. W. Yu, Hong Sun, and Jones T. K. Wan, Physica B **279**, 78 (2000).